SLAC-TN-07-003

North RTL 'Grid Scan' Studies

Stanford Linear Accelerator Center, Stanford University, Stanford, CA 94309

Work supported by Department of Energy contract DE–AC02–76SF00515.

SLAC-CN-381

AUTHOR: P. Emma
AFFILIATION: STANFORD LINEAR ACCELERATOR CENTER
DATE: October 17, 1990
TITLE: NORTH RTL "GRID SCAN" STUDIES*

Introduction

This study was made in response to screen measurements which indicated an emittance growth of nearly a factor of two within the North RTL or linac girder-1. Betatron oscillations are induced at the beginning of the North RTL to search for gross geometric aberrations arising within the RTL or sector-2 of the linac. The oscillations are induced horizontally and vertically with two *X* or two *Y* dipole correctors stepped in a nested loop fashion. In both cases the full set of RTL and first girder sector-2 linac beam position monitors (BPMs) are sampled in *X* and *Y* for each corrector setting. Horizontal (or vertical) data from pairs of BPMs are then transformed to phase space coordinates by the linear transformation constructed assuming the transport optics between the BPMs is known. A second transformation is then made to *normalized phase space* coordinates by using Twiss parameters consistent with the assumed transport optics. By careful choice of initial Twiss parameters the initial grid can be made square for convenience in graphical interpretation. A linear "grid" is then fitted to the transformed data points for each pair of BPMs. The area of each grid is calculated and linearity qualitatively evaluated. Furthermore, although not the focus of this study, the beta match at each BPM can be quantified.

Data Acquisition

Data sets were recorded on two separate occasions; the first set concentrated on the RTL, and the second set focused on the RTL-linac transition. In both instances the bunch compressor was turned off to minimize energy spread, and the end-of-RTL launch feedback was switched off. The RTL was first steered smooth (200 μm RMS) and the long RTL loss monitor was continually checked to verify no beam loss had occurred. The correctors used are just a few feet downstream of the damping ring extraction septum. Each of the two correctors were scanned through 7 steps in nested loop fashion so that 49 different trajectories were recorded. To reduce statistical errors, each BPM reading was averaged over 5 beam pulses. The corrector amplitude was set to give roughly a 3 mm peak excursion in the RTL. This corresponds to a peak-to-peak swing of ~8 times the RMS beam size.

DATA SET #1	Intensity:	3.0E10/bunch (1 bunch)
	Correctors:	XCOR DR13 60 & 80 (hor), YCOR DR13 34 & 78 (ver)
	BPMs:	DR13 56 (NRTL beg.) to DR13 890 (NRTL end); 27 BPMs
	Date:	18-AUG-1990 11:00 AM
DATA SET #2	Intensity:	1.0E10/bunch (1 bunch)
	Correctors:	XCOR DR13 60 & 80 (hor), YCOR DR13 34 & 78 (ver)
	BPMs:	DR13 160 (dnstr of comp) to LI02 211 (sector 2); 27 BPMs
	Date:	24-AUG-1990 02:40 AM

*Work supported by Department of Energy contract DE-AC03-76SF00515.

K = SLC Group
SLAC, '90

12

13P

Analysis

The linear transformation used to obtain normalized phase space coordinates is

$$\begin{bmatrix} u_1 \\ v_1 \end{bmatrix} = \begin{bmatrix} \frac{1}{\sqrt{\varepsilon\beta_1}} & 0 \\ \frac{\alpha_1}{\sqrt{\varepsilon\beta_1}} & \sqrt{\frac{\beta_1}{\varepsilon}} \end{bmatrix} \begin{bmatrix} 1 & 0 \\ R_{11}^{(1:2)} & R_{12}^{(1:2)} \end{bmatrix}^{-1} \begin{bmatrix} x_1 \\ x_2 \end{bmatrix}, \qquad \text{(Eq. 1)}$$

where x_1 and x_2 are the position data from the current BPM pair which are separated by one BPM to optimize the phase advance (see Fig 1). The mean of the 49 trajectories is subtracted off, so these are actually difference trajectories. $R^{(1:2)}$ is the transfer matrix between BPM-1 & 2, α_1 and β_1 are Twiss parameters at BPM-1 (see below), ε is the nominal RTL beam emittance (6800 μm-μrad), and u_1 and v_1 are the desired normalized phase space coordinates at BPM-1. Including the emittance in the normalization conveniently scales the u,v coordinates so that the units are nominal RMS beam size. This transformation is applied to each of the 49 points per BPM pair and v_1 is plotted versus u_1 to form a grid of points. This grid construction is repeated over each of ~20 BPM pairs.

The transfer matrices are taken from the SLC Data Base after an on-line model run. The Twiss parameters used are the propagation of the chosen initial Twiss parameters, α_0 and β_0 through the proper transfer matrix elements.

$$\begin{bmatrix} \alpha_1 \\ \beta_1 \\ \gamma_1 \end{bmatrix} = \begin{bmatrix} R_{11}^2 & -2R_{11}R_{12} & R_{12}^2 \\ -R_{11}R_{21} & 1+2R_{12}R_{21} & -R_{12}R_{22} \\ R_{21}^2 & -2R_{21}R_{22} & R_{22}^2 \end{bmatrix} \begin{bmatrix} \alpha_0 \\ \beta_0 \\ \gamma_0 \end{bmatrix} \qquad \text{(Eq. 2)}$$

Here the R matrix transports from the chosen initial point (BPM-0) to the first BPM of the current pair (BPM-1). The initial Twiss parameters are chosen so that the first BPM pair produces a square grid (see appendix). The choice of correctors is then less restricted. It is only required that they be a non-degenerate set ($\Delta\psi \neq n\pi$). A linear grid is then fitted to the transformed data points using the known corrector kick angles θ_1 and θ_2 as a parametrization.

$$\begin{aligned} u_1(t) &= a\theta_1(t) + b\theta_2(t) \\ v_1(t) &= c\theta_1(t) + d\theta_2(t) \end{aligned} \qquad \text{(Eq. 3)}$$

The fit coefficients (a, b, c, and d) are used only to evaluate a fitted u_1 and v_1 at each of the 49 points, therefore the absolute scale of the kick angles is irrelevant. The transformed data points and the fitted points are then superimposed on the same plot. The fitted points are connected by lines to form the grid, and the transformed points are represented as dots (*eg.* Figs 2). The area of the grid is calculated (see appendix) and normalized to the area at

BPM-0. In the absence of acceleration, which is the case for all of this data, the normalized area should remain unity as the BPM pairs move down the beam line.

Results

Data set #1 shows no clear measurable geometric aberrations anywhere in the RTL (Figs 2), and the normalized area remains unity to within an RMS of 8.6% (Fig 3). The grids skew and stretch somewhat through the RTL indicating a probable beta matching problem. For completeness the beta match is calculated (see appendix for definition) and is displayed for each grid in Figs 2 & 4. However, matching was not the focus of this study. It is being addressed in a separate study with a transfer matrix reconstruction technique using the same data.

Data set #2 also shows no measurable geometric aberrations within the RTL or the linac (Figs 4). The magnitude of the oscillations in data set #2 was smaller than data set #1 and therefore there appears more scatter in the RTL grids of Figs 4. Note, however, that the grid area increases step-wise by ~40% at the RTL/linac transition (Fig 5). This cannot be attributed to a focusing error, since focusing errors will skew the grid but will not affect the grid area (see appendix). Cross plane coupling was excluded by the results an independent transfer matrix reconstruction technique which fitted no off diagonal coupling terms in the 4×4 transfer matrix. Furthermore, the points fit very well to a linear grid in the linac (*eg.* bottom two grids of Figs 4), so no geometric aberration is measurable. The probable explanation of the area step is that there exists a relative BPM calibration error between the RTL and linac BPMs. An empirical fudge of 1.18 done to the linac BPM scaling factors in Feb. '89 will account for this 40% discrepancy ($1.18^2 = 1.39$). With this BPM calibration error accounted for, the normalized area also remains unity to within an RMS of 5.4%.

A third data set was also taken using north damping ring correctors to explore the extraction septum fields. This analysis will be described in a separate note. The grid produced, however, provides a good example of a measurable geometric effect (Fig 6). It should be noted that the septum is upstream of the first screen which was used to measure the factor of two emittance growth.

Conclusions

For the North RTL/linac data presented here:

- No measurable geometric aberrations are seen in the North RTL or girder-1/sector-2 of the linac.
- A probable relative BPM calibration error of 18±2 % exists between the North RTL and linac sector-2 BPMs

The grid technique has advantages over simply comparing a measured oscillation with a model. The oscillation comparison does not assume an area preserving map and, for example, may confuse a BPM calibration error with a focusing error. Furthermore, since it does not force linearity, the grid technique will show any nonlinearities over the scan range and so the technique is useful for qualitatively evaluating geometric effects.

Acknowledgements

I wish to acknowledge the numerous helpful discussions I have had with Bill Spence. Many of the techniques used in the appendix were learned from him and for this I am very grateful. I also credit Max Cornacchia for suggesting grid scanning as a diagnostic tool.

APPENDIX

Assume the initial transformation from x_1, x_2 to x_1, x_1' has been applied and begin in these phase space coordinates. The normalized phase space transformation is straight forward, with the exception of the initial BPM (BPM-0). Normalized phase space at BPM-0 is obtained by the transformation

$$\vec{u}_0 = (\sqrt{\varepsilon}\mathbf{A}_0)^{-1}\vec{x}_0 \,. \qquad \text{(Eq A1)}$$

$$\mathbf{A}_0 \equiv \frac{1}{\sqrt{\beta_0}}\begin{bmatrix} \beta_0 & 0 \\ -\alpha_0 & 1 \end{bmatrix}; \qquad \vec{u}_0 \equiv \begin{bmatrix} u_0 \\ v_0 \end{bmatrix}, \qquad \vec{x}_0 \equiv \begin{bmatrix} x_0 \\ x_0' \end{bmatrix} \qquad \text{(Eqs A2)}$$

For the grid scan graphics it is convenient to **choose** the Twiss parameters at BPM-0 in order to produce an initially square grid. The actual *beam* Twiss parameters may also be used, however the grids will not be square initially so that downstream optical distortions, when they occur, will be more difficult to discern.

The initial Twiss parameters are chosen by finding the transformation matrix $\mathbf{M}$, from x_0, x_0' which 'squares' the initial grid while maintaining its area. From the left of Fig A1, this suggests the three equations

$$\mathbf{M}\vec{p}_0 = a\begin{bmatrix} 1 \\ 0 \end{bmatrix}; \qquad \mathbf{M}\vec{q}_0 = a\begin{bmatrix} 0 \\ 1 \end{bmatrix}; \qquad \det(\mathbf{M}) = 1 \,. \qquad \text{(Eqs A3)}$$

Here a is a scale factor adjusted so that the area is unchanged, and the vectors p_0 and q_0 are indicated in Fig A1. The transformation $\mathbf{M}$ is then calculated as

$$\mathbf{M} = \sqrt{|\det(\mathbf{G}_0)|}\;\mathbf{G}_0^{-1}; \qquad \mathbf{G}_0 \equiv [\vec{p}_0 \quad \vec{q}_0] = \begin{bmatrix} p_1 & q_1 \\ p_2 & q_2 \end{bmatrix}. \qquad \text{(Eqs A4)}$$

Since p_0 and q_0 are 2-dimensional column vectors, $\mathbf{G}_0$ is a 2×2 matrix, as is $\mathbf{M}$. The grid area S_0 is calculated as the cross product magnitude

$$S_0 = |\vec{p}_0 \times \vec{q}_0| = |\det(\mathbf{G}_0)| \,. \qquad \text{(Eq A5)}$$

Substituting $\mathbf{M}$ for $\mathbf{A}_0$ into Eq A1 would provide a square grid with unchanged area (except for the ε factor) at BPM-0. However, $\mathbf{M}$ is not necessarily lower triangular and therefore identification of the elements of $\mathbf{M}$ as the chosen Twiss parameters is difficult. To convert $\mathbf{M}$ into a lower triangular matrix, we simply rotate it through the angle θ with the orthogonal matrix $\mathbf{O}$ (equivalent to defining the initial betatron phase advance)*

---

* This technique was suggested by Bill Spence

$$\mathbf{OM} = \begin{bmatrix} \cos\theta & \sin\theta \\ -\sin\theta & \cos\theta \end{bmatrix} \mathbf{M} = \begin{bmatrix} \beta_0^{-\frac{1}{2}} & 0 \\ \alpha_0\beta_0^{-\frac{1}{2}} & \beta_0^{\frac{1}{2}} \end{bmatrix} \qquad \text{(Eq A6)}$$

The angle θ is solved using $(\mathbf{OM})_{12} = 0$, and the initial Twiss parameters follow.

$$\tan\theta = -\frac{\mathbf{M}_{12}}{\mathbf{M}_{22}} \qquad \beta_0 = (\mathbf{OM})_{11}^{-2} \qquad \alpha_0 = \frac{(\mathbf{OM})_{21}}{(\mathbf{OM})_{11}} \qquad \text{(Eqs A7)}$$

Calculating the Twiss parameters at the other BPMs then reduces to application of Eq 2. The transformation to normalized phase space at a downstream BPM pair follows as in A1.

$$\vec{u}_1 = (\sqrt{\varepsilon}\mathbf{A}_1)^{-1}\vec{x}_1 \qquad \text{(Eq A8)}$$

Now express phase space at BPM-1 in terms of that at BPM-0 as

$$\vec{x}_1 = \mathbf{R}^{(0:1)}\vec{x}_0\,, \qquad \text{(Eq A9)}$$

and decompose the transfer matrix $\mathbf{R}$ into initial and final Twiss parameters and an orthogonal rotation matrix Ψ (betatron phase advance).

$$\mathbf{R}^{(0:1)} = \mathbf{A}_1\Psi_{01}\mathbf{A}_0^{-1}\,; \qquad \Psi_{01} \equiv \begin{bmatrix} \cos\Delta\psi & \sin\Delta\psi \\ -\sin\Delta\psi & \cos\Delta\psi \end{bmatrix} \qquad \text{(Eqs A10)}$$

The Twiss matrices $\mathbf{A}_1$ and $\mathbf{A}_0$ are as defined in the first of Eqs A2, and $\Delta\psi$ is the betatron phase advance from BPM-0 to BPM-1.

Examining the effect of a focusing error between BPM-0 and BPM-1, we note that this error will change the final Twiss parameters and the phase advance between BPM-0 and BPM-1. The effect of a focusing error on the transfer matrix can be written as

$$\hat{\mathbf{R}}^{(0:1)} = \hat{\mathbf{A}}_1\hat{\Psi}_{01}\mathbf{A}_0^{-1}\,, \qquad \text{(Eq A11)}$$

where the 'hatted' (measured) matrices are introduced to distinguish them from the model matrices. Combining A8, A9, A11, and A1 gives

$$\vec{u}_1 = (\sqrt{\varepsilon}\mathbf{A}_1)^{-1}\hat{\mathbf{A}}_1\hat{\Psi}_{01}\mathbf{A}_0^{-1}\vec{x}_0 = \left(\mathbf{A}_1^{-1}\hat{\mathbf{A}}_1\right)\hat{\Psi}_{01}\vec{u}_0\,. \qquad \text{(Eqs A12)}$$

From A12 it is clear that in the absence of a focusing error ($\hat{\mathbf{A}}_1 = \mathbf{A}_1$) the grid at BPM-1 is simply a clockwise rotation of the grid at BPM-0 through $\Delta\psi > 0$. Furthermore, since the determinants of all matrices in Eqs A12 are unity, the grid area is invariant and independent of the choice of initial Twiss parameters.

The quality of the beta match is indicated in the 'squareness' of the grid. The 'squareness' of each grid will be defined as the sum of the squares of the lengths of the grid spanning vectors h_1 and k_1 at BPM-1 (as is shown for BPM-0 in Fig A1) which are taken from the grid fit. Writing the grid as a 2×2 matrix of these two vectors

$$\mathbf{H}_1 = \left[\vec{h}_1 \;\; \vec{k}_1\right], \qquad \text{(Eq A13)}$$

the 'squareness' can then be conveniently written as the trace of $\mathbf{H}_1$ times itself transposed.

$$\mathrm{tr}(\mathbf{H}_1\mathbf{H}_1^T) = \left|\vec{h}_1\right|^2 + \left|\vec{k}_1\right|^2 \qquad \text{(Eq A14)}$$

From A3, A4, and A6, $\mathbf{H}_0$ can be written as

$$\mathbf{H}_0 \equiv \left[\vec{h}_0 \;\; \vec{k}_0\right] = \sqrt{\left|\det(\mathbf{G}_0)\right|}\,\mathbf{O}\,. \qquad \text{(Eq A15)}$$

Transformation from $\mathbf{H}_0$ to $\mathbf{H}_1$ is the same as transformation from u_0 to u_1 in A12

$$\mathbf{H}_1 = \left(\mathbf{A}_1^{-1}\widehat{\mathbf{A}}_1\right)\widehat{\Psi}_{01}\mathbf{H}_0 \equiv \mathbf{F}_1\mathbf{H}_0\,, \qquad \text{(Eq A16)}$$

where the definition of $\mathbf{F}_1$ is here implicit. Rewriting A14 using A16 and A15 gives the 'squareness' in terms of $\mathbf{F}_1$.

$$\mathrm{tr}\left(\mathbf{H}_1\mathbf{H}_1^T\right) = \mathrm{tr}\left(\mathbf{F}_1\mathbf{H}_0\mathbf{H}_0^T\mathbf{F}_1^T\right) = \left|\det(\mathbf{G}_0)\right|\,\mathrm{tr}\left(\mathbf{F}_1\mathbf{F}_1^T\right) \qquad \text{(Eq A17)}$$

Substituting $\mathbf{A}_1$ and its 'hatted' counterpart into the definition of $\mathbf{F}_1$ produces a beta match parameter, ζ, in terms of the Twiss parameters at BPM-1 of the current pair, which is invariant until the next focusing error is encountered.

$$\begin{aligned}\zeta \equiv \frac{1}{2}\mathrm{tr}\left(\mathbf{F}_1\mathbf{F}_1^T\right) &= \frac{1}{2}\mathrm{tr}\left\{\left(\mathbf{A}_1^{-1}\widehat{\mathbf{A}}_1\right)\widehat{\Psi}_{01}\widehat{\Psi}_{01}^T\left(\mathbf{A}_1^{-1}\widehat{\mathbf{A}}_1\right)^T\right\} = \\ &\frac{1}{2}\mathrm{tr}\left\{\left(\mathbf{A}_1\mathbf{A}_1^T\right)^{-1}\left(\widehat{\mathbf{A}}_1\widehat{\mathbf{A}}_1^T\right)\right\} = \frac{1}{2}\mathrm{tr}\left(\sigma_1^{-1}\widehat{\sigma}_1\right) = \\ &\frac{1}{2}\left\{\frac{\beta_1}{\widehat{\beta}_1} + \frac{\widehat{\beta}_1}{\beta_1} + \beta_1\widehat{\beta}_1\left(\frac{\alpha_1}{\beta_1} - \frac{\widehat{\alpha}_1}{\widehat{\beta}_1}\right)^2\right\}\end{aligned} \qquad \text{(Eq A18)}$$

The factor of 1/2 is introduced so that the matched case will result in $\zeta = 1$, and the beam matrix, σ, is introduced, which follows from

$$\mathbf{A}\mathbf{A}^T = \begin{bmatrix}\beta & -\alpha \\ -\alpha & \gamma\end{bmatrix} \equiv \frac{\sigma}{\varepsilon}\,, \qquad \text{(Eq A19)}$$

and the following matrix properties are employed

$$\mathrm{tr}(\mathbf{ABC}) = \mathrm{tr}(\mathbf{CAB}), \qquad (\mathbf{AB})^{\mathrm{T}} = \mathbf{B}^{\mathrm{T}}\mathbf{A}^{\mathrm{T}}, \qquad (\mathbf{AB})^{-1} = \mathbf{B}^{-1}\mathbf{A}^{-1}.$$

This beta match parameter is actually the amplitude of a beta beat which can also be written

$$\zeta = \left(1 + \left\|\frac{\Delta\beta}{\beta}\right\|^2\right)^{\frac{1}{2}}, \qquad \text{(Eq A20)}$$

where $\|\Delta\beta/\beta\|$ is the fractional beta beat amplitude. The 'hatted' quantities in A18 represent the measured parameters, while those without the 'hats' represent the design. From A14, A17, and A18, the beta beat amplitude, ζ, at BPM-1 of each BPM pair (indicated at the bottom of each grid in Figs 2 and Figs 4), is a direct result of the fitted grid vectors h_1 and k_1.

$$\zeta = \frac{1}{2}\frac{|\vec{h}_1|^2 + |\vec{k}_1|^2}{|\det(\mathbf{G}_0)|} \qquad \text{(Eq A21)}$$

A quick proof of the invariance of ζ can be made by calculating ζ_i at a point downstream, if we transport both the design beam, σ and the "measured" beam, $\hat{\sigma}$ to point-i through the same $\mathbf{R}$ and use the previous matrix properties.

$$\zeta_i = \frac{1}{2}\mathrm{tr}\left\{\left(\mathbf{R}\sigma\mathbf{R}^{\mathrm{T}}\right)^{-1}\left(\mathbf{R}\hat{\sigma}\mathbf{R}^{\mathrm{T}}\right)\right\} =$$
$$\frac{1}{2}\mathrm{tr}\left\{\left(\mathbf{R}^{-1}\mathbf{R}\right)^{\mathrm{T}}\sigma^{-1}\left(\mathbf{R}^{-1}\mathbf{R}\right)\hat{\sigma}\right\} = \frac{1}{2}\mathrm{tr}\left\{\sigma^{-1}\hat{\sigma}\right\} = \zeta \qquad \text{(Eq A22)}$$

As a final point, it should be noted that although the choice of initial Twiss parameters at BPM-0 does not affect the invariance of ζ, this choice does affect the step size of ζ when a focusing error is encountered. Therefore, the Twiss parameters of the beam itself should be used at BPM-0 (rather than the grid squaring Twiss parameters as used in Figs 2 & 4) if a directly qualitative beta matching study were of prime interest.

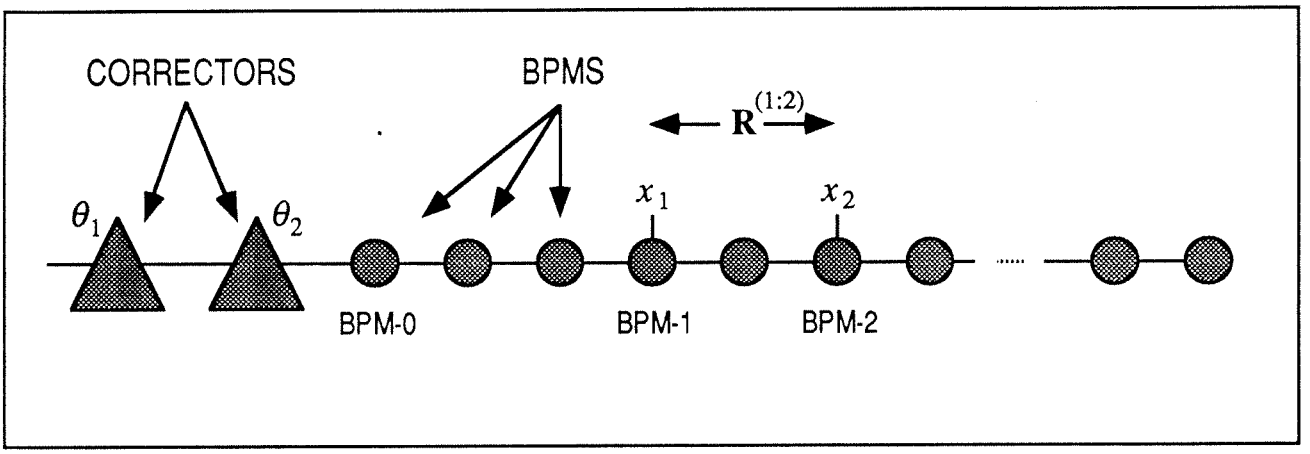

Fig 1. Corrector/BPM relationship (an arbitrary BPM pair is shown as an example).

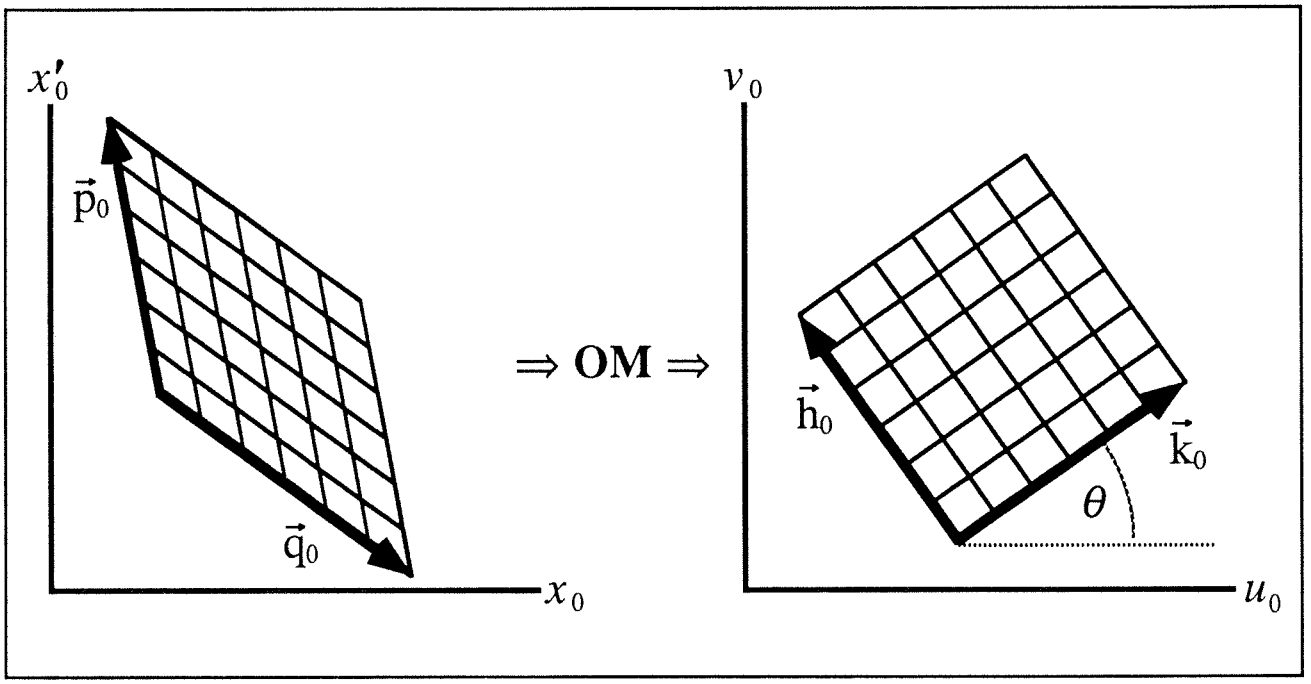

Fig A1. Grid *squaring* at the initial BPM (BPM-0)

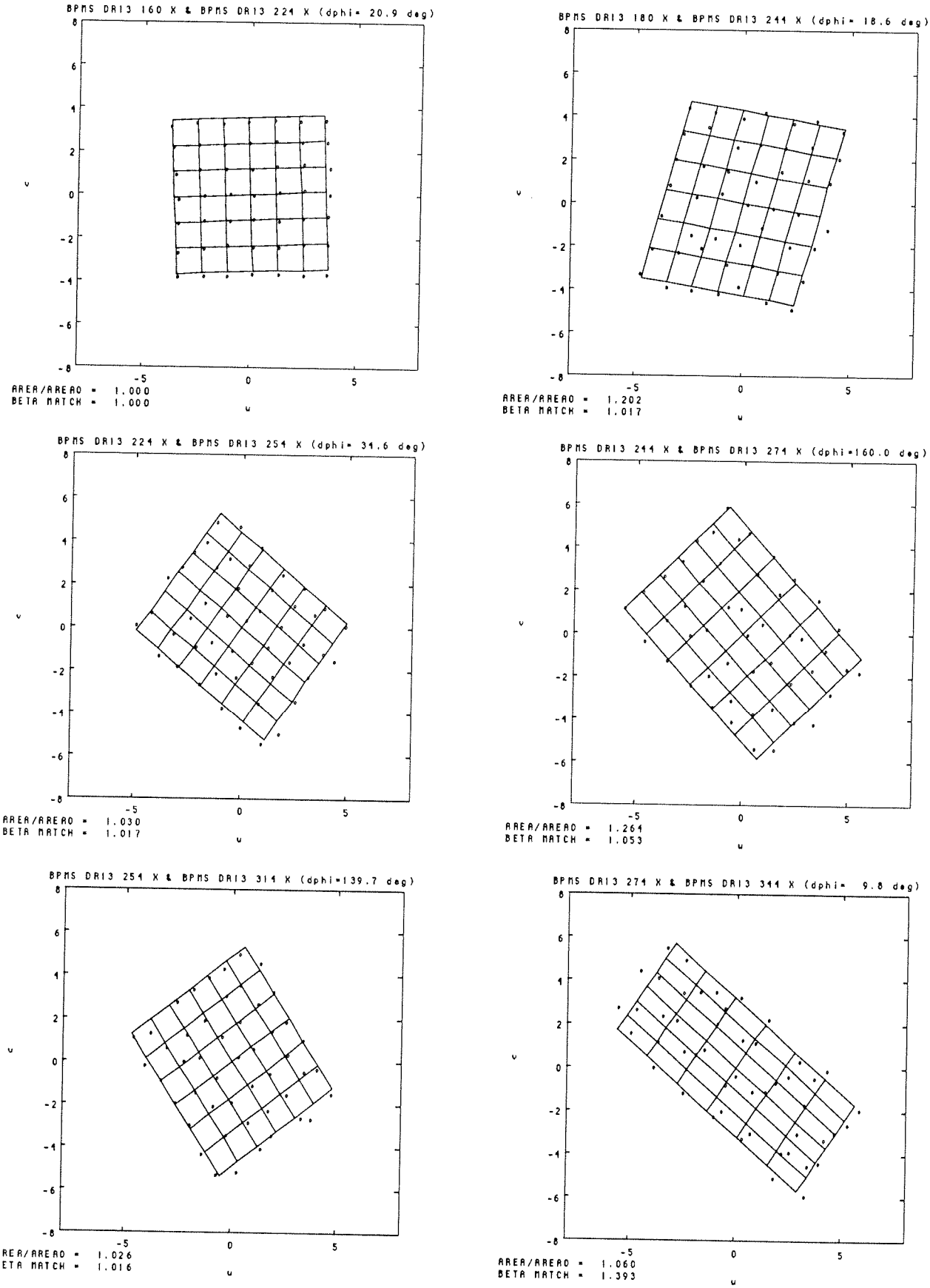

Figs 2. North RTL grids (data set #1)

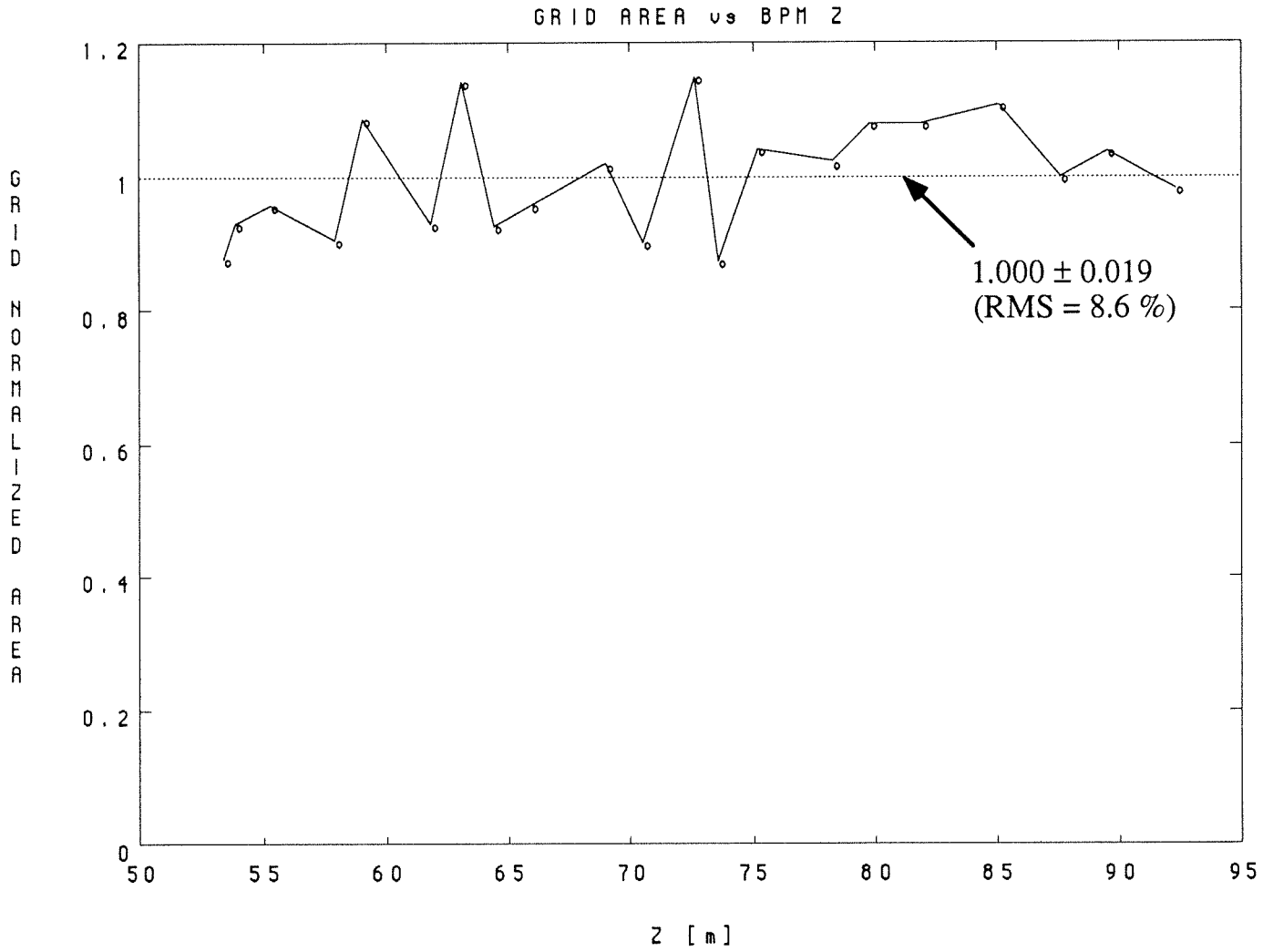

Fig3. Normalized RTL grid area vs BPM Z-position (data set #1)

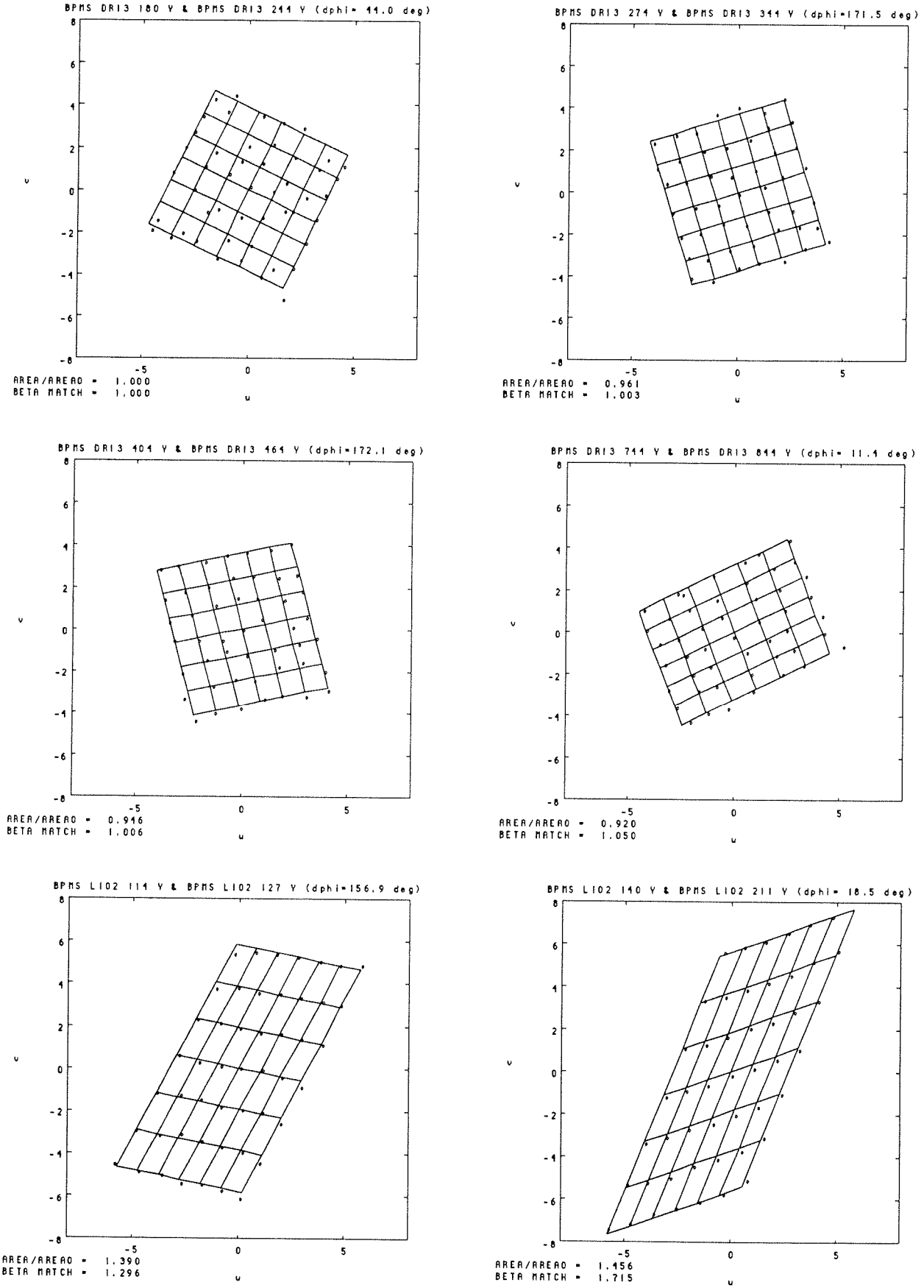

Figs 4. North RTL and linac sector 2 grids (data set #2)

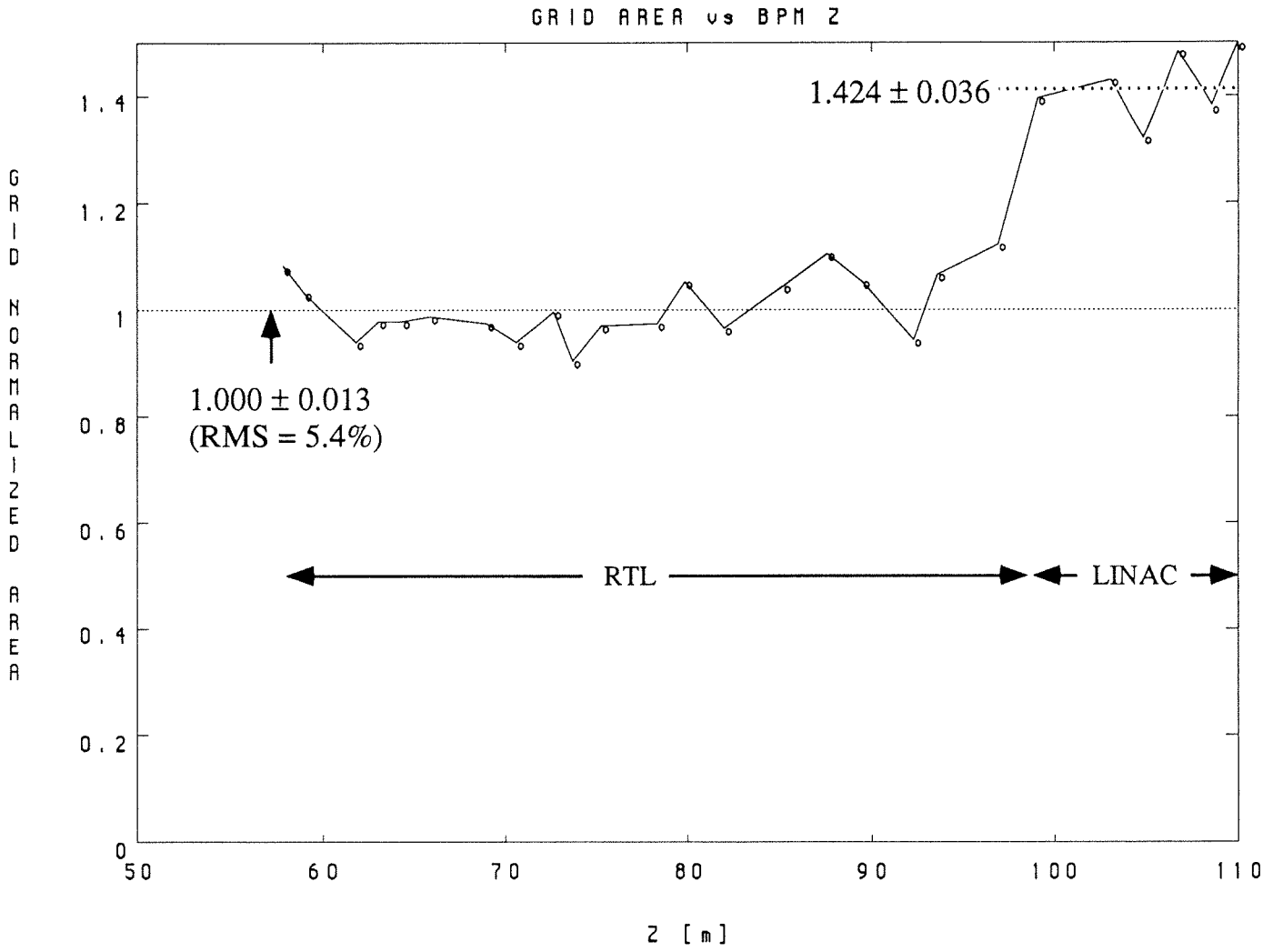

Fig 5. Grid area vs Z with sudden increase of ~40% at RTL/linac transition (data set #2)

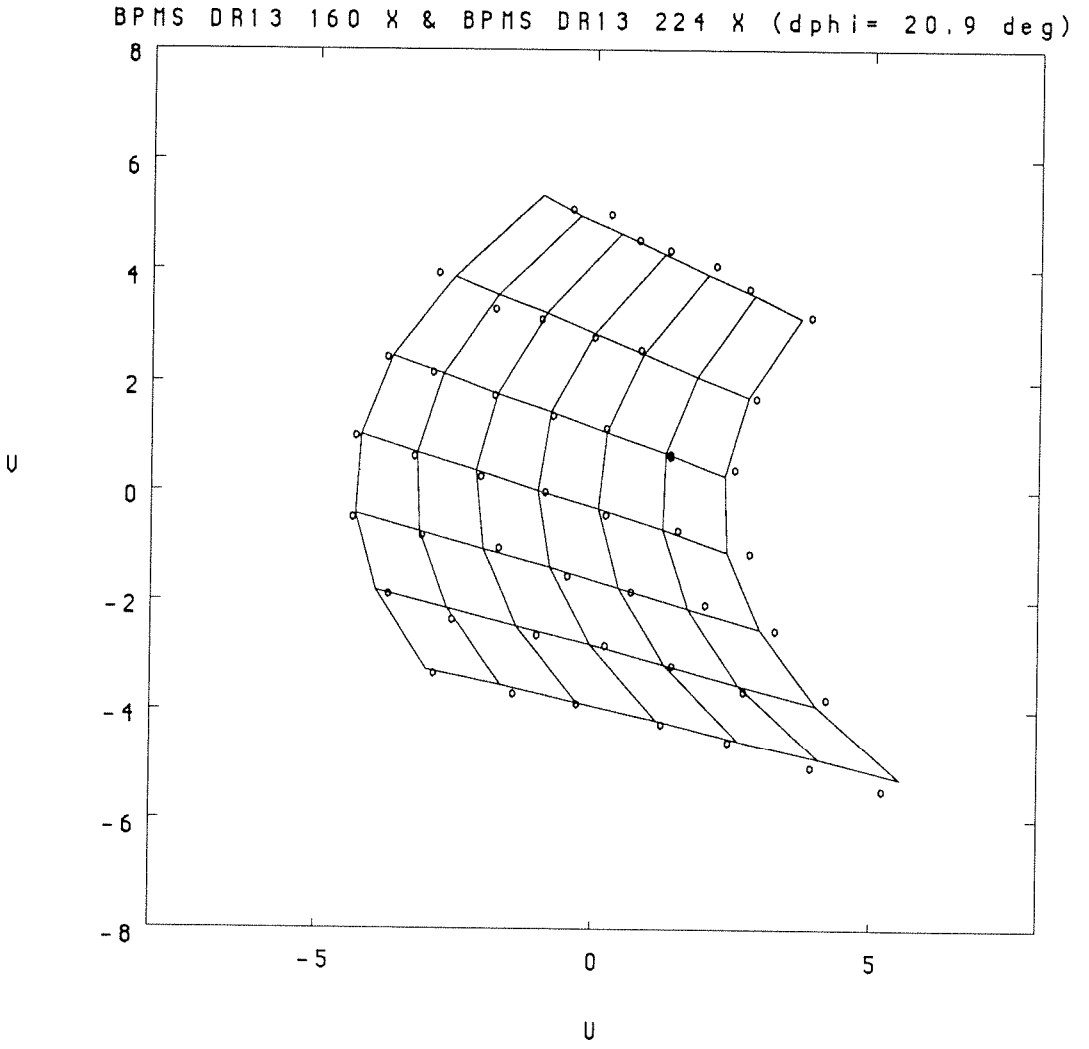

Fig 6. North damping ring extraction septum horizontal grid scan just downstream of the RTL compressor (grid fitted to second order).

Louise Addis
SLAC Bin 82

C
A
1